

GEOCHEMICAL CHARACTERISTICS OF GOLD MINERALIZATION AT TAUNG NI GOLD PROSPECT, MADAYA TOWNSHIP, MANDALAY REGION, MYANMAR

Aung Ye Ko¹, Day Wa Aung², Ohn Thwin³ and May Thwe Aye⁴

Abstract

Taung Ni gold prospect area is situated in Madaya Township, Mandalay Region, Myanmar. The host rocks, quartzite and phyllite were metamorphosed under greenschist facies conditions. Gold mineralization is mainly hosted by quartzite of Chaungmagyi Group which is deformed, jointed, brecciated and interbedded with phyllite. In its area, gold-bearing sulphide quartz veins and auriferous deformed/ remobilized quartz veins are found. In these two types of veins systems, Pearson statistical analyses confirm a significant correlation between SiO₂ and other major oxides as most strongly negative correlation indicates that the both quartz veins bearing gold are of hydrothermal origin. The Co and Ni contents in pyrite show Co>Ni and the average ratio for Co/Ni is 2.698. The gold fineness shows two ranges: (1) high fineness (826.2 - 881.3) and (2) low fineness (771 - 795). In sulphide bearing quartz vein (Early Stage), homogenization temperature can be measured and it ranges from 340°C to 403°C and melting temperature ranging from -1.7 to -2.0, salinity NaCl equiv. wt.% range from 3.01 to 3.53. In deformed quartz vein (Later Stage), the range of melting temperature is from -1.3 °C to -1.6 °C and salinity NaCl equiv. wt. % is from 2.31 to 2.83. Homogenization temperature is 320°C to 396°C.

Keywords – Taung Ni gold prospect, gold-bearing quartz veins, Co and Ni ratio, gold fineness, fluid inclusion microthermometry.

Introduction

Taung Ni area is situated in Madaya Township, Mandalay Region, Myanmar. It is located approximately 47 km to the northeast of Mandalay, and about 35 km northwest of Pyin-Oo-Lwin. It lies partly in Mogok Metamorphic Belt (MMB) and between the Sagaing Fault in the west and the Shan Scarp Fault in the east. The area occupies the western marginal zone of Shan Plateau and to the east of the Central Myanmar Basin. Location map of the study area is shown in Figure.1.

Aim and Methods of Study

The major purpose of this research is to elucidate significant anomalies, determine their relationships, use correlation analyses and assess mineralization zones so as to determine the origin of mineralization such as magmatic, hydrothermal, sedimentary or metamorphic. This research consists of two main stages, field work and laboratory work. During the field work, quartz veins samples and ore samples were collected from the quartz veins in the mineralization zone and the laboratory work consists of Atomic Absorption Spectrophotometry (AAS) and X-ray Fluorescence (XRF) methods, and ore microscopy, Scanning Electron Microscopy (SEM) - Energy-Dispersive X-ray Analyzer (EDX) analysis and Fluid inclusion microthermometry.

¹ Ph.D Candidate, Department of Geology, University of Yangon, Myanmar

² Dr, Professor & Head, Department of Geology, University of Yangon, Myanmar

³ Dr, Part-Time Professor, Department of Geology, University of Yangon, Myanmar

⁴ Dr, Professor, Department of Geology, University of Yangon, Myanmar

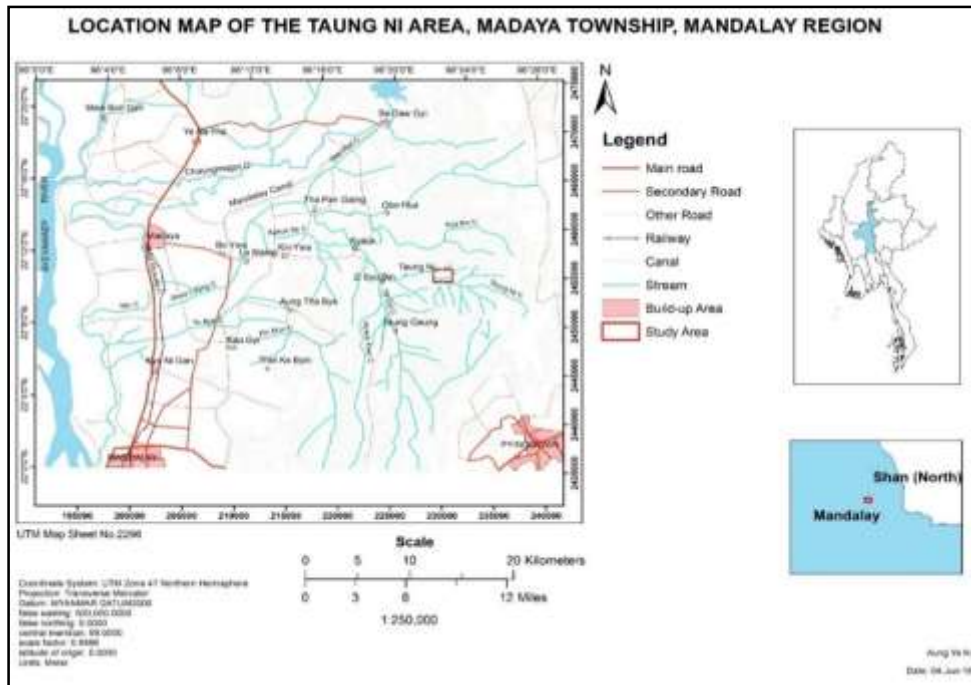


Figure1 Location Map of the Taung Gaung Area, Madaya Township, Mandalay Region

Deposit Geology

The study area, falling in the Shan-Thai Block, lies in the eastern margin of Mogok Metamorphic Belt (MMB) and between the Sagaing Fault in the west and the Shan Scarp Fault in the east. It occupies the western marginal zone of Shan Plateau to the east of the Central Myanmar Basin. The MMB consists of metamorphosed sedimentary sequences of Precambrian to Carboniferous age. Basement sediments are intruded by Jurassic to Tertiary age granitoids. Stratigraphic rock units include Mogok Group, Chaungmagyi Group, Panguyun Group, Naungkangyi Group and Upper Plateau Limestone.

The geology of the Taung Ni area is quite simple. There is only one stratigraphic rock units in this area. It is Upper Precambrian to Lower Cambrian age of Chaungmagyi Group, consisting of Mauk Kaw Quartzite and Kin Sandy Phyllite (Khin Maung Shwe, 1973) (Figure 2). On the basis of microscopic study and XRD results, quartzite and phyllite were composed of low-grade metamorphic minerals such as albite, quartz, chlorite, sericite, epidote, muscovite, actinolite, and biotite. Opaque minerals were often found as disseminations especially observed in phyllite with foliations resulting from the sub-parallel to parallel orientation of minerals such as chlorite or micas due to strong pressure conditions of metamorphism. Therefore, this rock type has been formed by low grade regional metamorphism. The common occurrence of chlorite and sericite suggest the low pressure and low temperature. It shows that this rock type is of the greenschist facies (Aung Ye Ko et al., 2018c).

The mineralization style of the study area is the designated vein type deposit hosted by quartzite of Chaungmagyi Group which is deformed, jointed and brecciated and interbedded with phyllite. The gold-bearing mineralized veins are mostly brecciated and crushed. The thickness of the auriferous quartz vein/ veinlets ranges from 1cm to 15cm which fill NE-SW and E-W structure lineaments of dilational fault zone. The main controlling factor is the regional structure that nearly trends NE-SW and possibly formed by the activity of Phayaung Taung Fault and cause the deformation like, shearing, brecciation favourable for mineralization. Gold is associated with pyrite, arsenopyrite, chalcopyrite, hematite, silver, gold, electrum, petzite, hessite and tellurobismuthite.

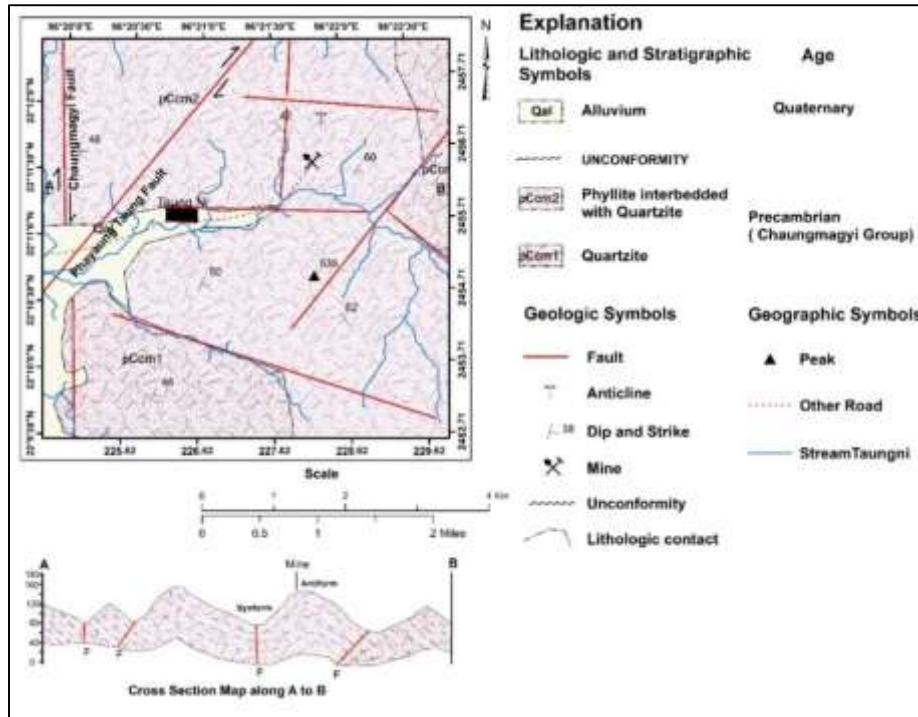


Figure 2 Geological Map of the Taung Ni Area and its environs, Madaya Township, Mandalay Region, Myanmar

Results and Discussion

Geochemistry of gold-bearing quartz veins

In Taung Ni area, two types of vein systems are found: (1) gold-bearing sulphide quartz veins and (2) auriferous deformed/remobilized quartz veins in strongly brecciated and oxidized zone (Figure. 3 & 4).

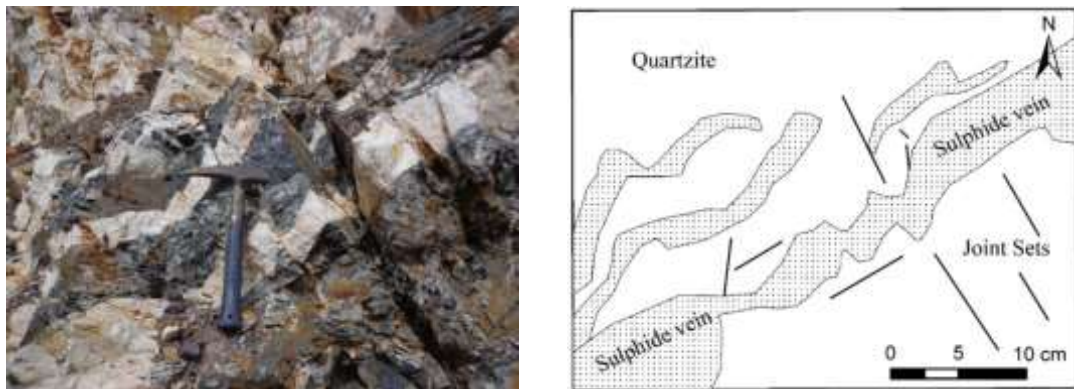


Figure 3 Individual vein system of sulphide quartz veins hosted in quartzite

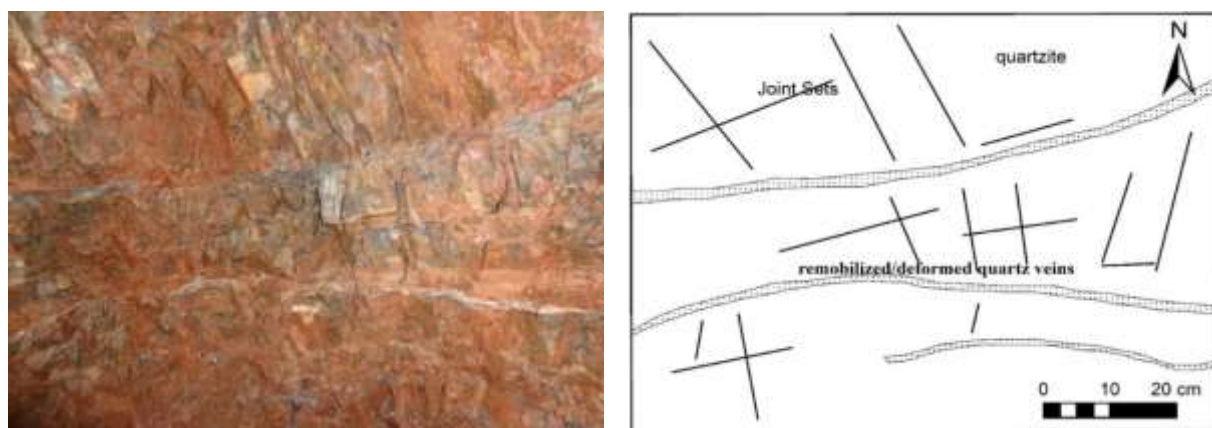


Figure 4 Individual vein system of deformed/remobilized quartz veins hosted in quartzite

In gold-bearing sulphide quartz veins, the whole rock geochemical composition of quartz vein with XRF method of analysis is shown in APPENDIX. The quartz veins are highly siliceous. The composition of SiO_2 varies from 89.81 to 99.68wt%, Al_2O_3 ranges from 0.05 to 2.23wt%, Fe_2O_3 is of the order of 0.07 to 6.26wt%, and MgO varies from 0.01to 1.23wt%, and the concentrations of other major oxides are very low.

Pearson statistical analyses confirm a strong negative correlation between SiO_2 and other major oxides (Table 1). The results indicate that the quartz veins were of hydrothermal origin. The Si-Al discrimination diagram is used to distinguish hydrothermal from sedimentary deposits (Peters, 1988). The ore samples in gold-bearing sulphide quartz veins are almost within the field of hydrothermal field (Figure 5).

The concentration of (Ni-Zn-Co) in quartz veins were plotted on ternary diagram which was used to differentiate between hydrothermal and sedimentary deposits (Figure 6). The data plotted indicate that the quartz veins bearing gold are of hydrothermal origin (Choi and Hariya, 1992).

The concentration of (Co+Ni+Cu+Zn)-Fe-Mn in quartz veins were plotted on ternary diagram which was used to differentiate between hydrothermal and sedimentary deposits (Figure 7). The data plotted indicate that the quartz veins bearing gold are of hydrothermal origin (Bonatti, Kraemer and Rydell, 1972c).

Table 1 Pearson correlation coefficient values of major oxides in gold-bearing sulphide quartz veins

| Proximity Matrix | | | | | | | | | | |
|-------------------------|-------------------|----------------|-------------------------|-------------------------|--------------|--------------|--------------|-----------------------|----------------------|------------------------|
| Case | Matrix File Input | | | | | | | | | |
| | SiO_2 | TiO_2 | Al_2O_3 | Fe_2O_3 | MnO | MgO | CaO | Na_2O | K_2O | P_2O_5 |
| SiO_2 | 1 | | | | | | | | | |
| TiO_2 | -0.506 | 1 | | | | | | | | |
| Al_2O_3 | -0.48 | 0.196 | 1 | | | | | | | |
| Fe_2O_3 | -0.954 | 0.581 | 0.209 | 1 | | | | | | |
| MnO | -0.845 | 0.327 | -0.035 | 0.933 | 1 | | | | | |
| MgO | -0.526 | 0.146 | 0.932 | 0.276 | 0.031 | 1 | | | | |
| CaO | -0.486 | 0.29 | 0.913 | 0.257 | -0.034 | 0.969 | 1 | | | |
| Na_2O | -0.007 | 0.125 | 0.326 | -0.089 | -0.117 | 0.016 | 0.08 | 1 | | |
| K_2O | 0.114 | -0.25 | -0.258 | -0.064 | 0.08 | -0.301 | -0.43 | -0.34 | 1 | |
| P_2O_5 | -0.897 | 0.082 | 0.443 | 0.81 | 0.802 | 0.557 | 0.44 | -0.13 | -0.04 | 1 |

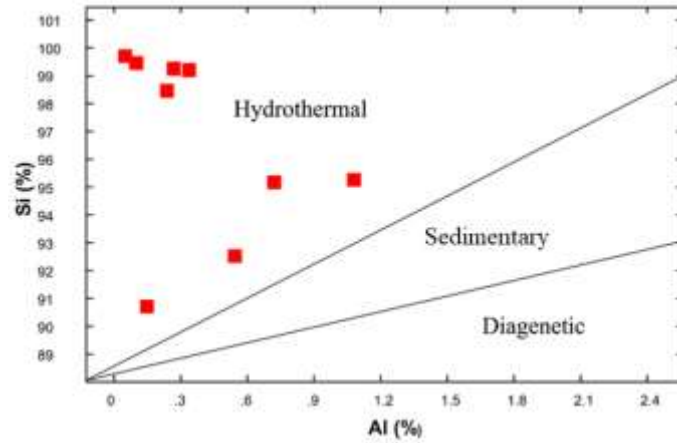


Figure 5 Si-Al discrimination diagram of gold-bearing sulphide quartz veins

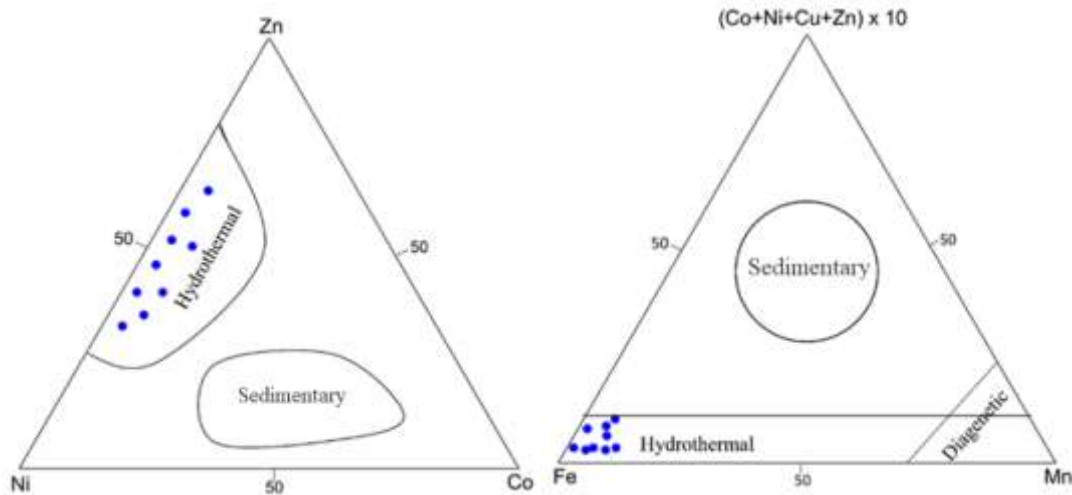


Figure 6 (Ni-Zn-Co) ternary plot of gold-bearing sulphide quartz veins

Figure 7 (Co+Ni+Cu+Zn)-Fe-Mn ternary plot of gold-bearing sulphide quartz veins

Au, Ag, As, Bi, Cu, Mo, Pb, S, Sb, Se and Te were analyzed by atomic absorption spectrometry (AAS). This method yields very high-quality data for these elements (Nurmi et al., 1991) with detection limits of 0.01ppm. The concentration of Au varies from 1.53 to 2.62 ppm, and the concentrations of associated elements in gold-bearing sulphide quartz veins are shown in Table 2. Pearson correlation coefficient values of Au and associated elements in gold-bearing sulphide quartz veins are shown in Table 3.

Table 2 The concentration of Au and associated elements in gold-bearing sulphide quartz veins

| | Au (ppm) | Ag (ppm) | As (ppm) | Bi (ppm) | Cu | Mo | Pb | S | Sb | Se | Te |
|--------|----------|----------|----------|----------|------|----|----|-----|------|-----|-----|
| TNQS-1 | 1.53 | 2.1 | 6 | 2.1 | 3560 | 42 | 4 | 0.1 | 0.7 | 0.2 | 150 |
| TNQS-2 | 1.75 | 1.3 | 3 | 1.97 | 2520 | 46 | 4 | 0.3 | 0.27 | 1.2 | 170 |
| TNQS-3 | 2.62 | 4.8 | 8 | 4.29 | 5400 | 36 | 5 | 1.2 | 0.56 | 1.3 | 230 |
| TNQS-4 | 2.59 | 4.5 | 7 | 3.36 | 5550 | 59 | 7 | 1.7 | 0.55 | 1.3 | 280 |
| TNQS-5 | 1.57 | 2.2 | 3 | 2.1 | 3210 | 47 | 3 | 1.1 | 0.52 | 0.5 | 120 |
| TNQS-6 | 1.65 | 1.2 | 4 | 1.81 | 4100 | 30 | 9 | 0.1 | 0.6 | 0.7 | 140 |
| TNQS-7 | 1.8 | 2.8 | 6 | 1.3 | 3220 | 32 | 4 | 0.2 | 0.5 | 1.2 | 100 |

Table 3 Pearson correlation coefficient values of Au and associated elements in gold-bearing sulphide quartz veins

| Proximity Matrix | | | | | | | | | | | |
|------------------|-------------------|-------|-------|-------|-------|--------|-------|-------|--------|-------|----|
| Case | Matrix File Input | | | | | | | | | | |
| | Au | Ag | As | Bi | Cu | Mo | Pb | S | Sb | Se | Te |
| Au | 1 | | | | | | | | | | |
| Ag | 0.912 | 1 | | | | | | | | | |
| As | 0.786 | 0.911 | 1 | | | | | | | | |
| Bi | 0.874 | 0.828 | 0.704 | 1 | | | | | | | |
| Cu | 0.857 | 0.826 | 0.818 | 0.832 | 1 | | | | | | |
| Mo | 0.324 | 0.308 | 0.11 | 0.318 | 0.209 | 1 | | | | | |
| Pb | 0.278 | 0.043 | 0.136 | 0.195 | 0.567 | -0.103 | 1 | | | | |
| S | 0.759 | 0.78 | 0.506 | 0.746 | 0.686 | 0.684 | 0.085 | 1 | | | |
| Sb | 0.002 | 0.227 | 0.49 | 0.161 | 0.463 | -0.185 | 0.321 | 0.009 | 1 | | |
| Se | 0.738 | 0.543 | 0.363 | 0.408 | 0.362 | 0.113 | 0.106 | 0.407 | -0.558 | 1 | |
| Te | 0.875 | 0.723 | 0.621 | 0.846 | 0.804 | 0.602 | 0.383 | 0.741 | 0.022 | 0.511 | 1 |

Ag, As, Bi, Cu, S, Se and Te are strongly correlated with Au (Table 3). These correlations show that the mineralization indicates the complex nature of hydrothermal system (Theodore et al., 1998). Although Mo, Pb and Sb are not closely associated with Au, Mo is moderately associated with Au, Ag, As, Bi, Cu, S, Se, Te, Pb and Sb are separate components. Bi, Te and Cu are strongly correlated with Au and Ag. As, Se and S are very well correlated with each other (Table 3). Analysis of the geological data from the gold-bearing sulphide quartz veins shows two distinct geological association: (1) Au, Ag, Bi, Te and Cu and (2) As, Se and S. Mo, Pb and Sb vary independent of each other and other associations.

In auriferous deformed/remobilized quartz veins, the whole rock geochemical composition of quartz vein was analyzed with XRF as shown in APPENDIX. The composition of SiO₂ varies from 83.78 to 96.58wt%, Al₂O₃ ranges from 1.6 to 9.15wt%, Fe₂O₃ is of the order of 0.65 to 3.49wt%, and MgO varies from 0.03 to 0.57wt%, and the concentrations of other major oxides are very low.

Pearson statistical analyses confirm a strong negative correlation between SiO₂ and other major oxides (Table 4). The results indicate that the quartz veins were of hydrothermal origin.

Fe and Mn are characteristically fractionated on precipitation from hydrothermal solution (Shah and Khan, 1999).

The Si-Al discrimination diagram is used to distinguish hydrothermal from sedimentary deposits (Peters, 1988). The ore samples in gold-bearing sulphide quartz veins are almost within the field of hydrothermal field (Figure 8).

The concentration of (Ni-Zn-Co) in quartz veins were plotted on ternary diagram which was used to differentiate between hydrothermal and sedimentary deposits (Figure 9). The data plotted indicate that the quartz veins bearing gold are of hydrothermal origin (Choi and Hariya, 1992).

The concentration of (Co+Ni+Cu+Zn)-Fe-Mn in quartz veins were plotted on ternary diagram which was used to differentiate between hydrothermal and sedimentary deposits (Figure 10). The data plotted indicate that the quartz veins bearing gold are of hydrothermal origin (Bonatti, Kraemer and Rydell, 1972c).

Table 4 Pearson correlation coefficient values of major oxides in auriferous deformed/remobilized quartz veins

| Proximity Matrix | | | | | | | | | | |
|------------------|-------------------|--------|--------|--------|--------|--------|--------|-------|-------|------|
| Case | Matrix File Input | | | | | | | | | |
| | SiO2 | TiO2 | Al2O3 | Fe2O3 | MnO | MgO | CaO | Na2O | K2O | P2O5 |
| SiO2 | 1 | | | | | | | | | |
| TiO2 | -0.804 | 1 | | | | | | | | |
| Al2O3 | -0.86 | 0.985 | 1 | | | | | | | |
| Fe2O3 | -0.942 | 0.901 | 0.939 | 1 | | | | | | |
| MnO | -0.062 | -0.3 | -0.318 | -0.205 | 1 | | | | | |
| MgO | -0.671 | 0.206 | 0.256 | 0.514 | 0.405 | 1 | | | | |
| CaO | -0.468 | -0.129 | -0.047 | 0.209 | 0.689 | 0.86 | 1 | | | |
| Na2O | -0.641 | 0.08 | 0.164 | 0.408 | 0.551 | 0.938 | 0.968 | 1 | | |
| K2O | -0.83 | 0.976 | 0.973 | 0.917 | -0.212 | 0.223 | -0.063 | 0.127 | 1 | |
| P2O5 | -0.418 | 0.497 | 0.55 | 0.351 | -0.297 | -0.055 | -0.128 | 0.026 | 0.455 | 1 |

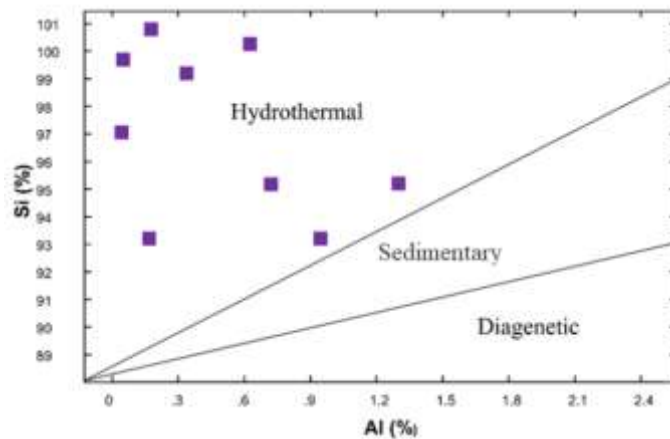


Figure 8 Si-Al discrimination diagram of auriferous deformed/ remobilized quartz veins

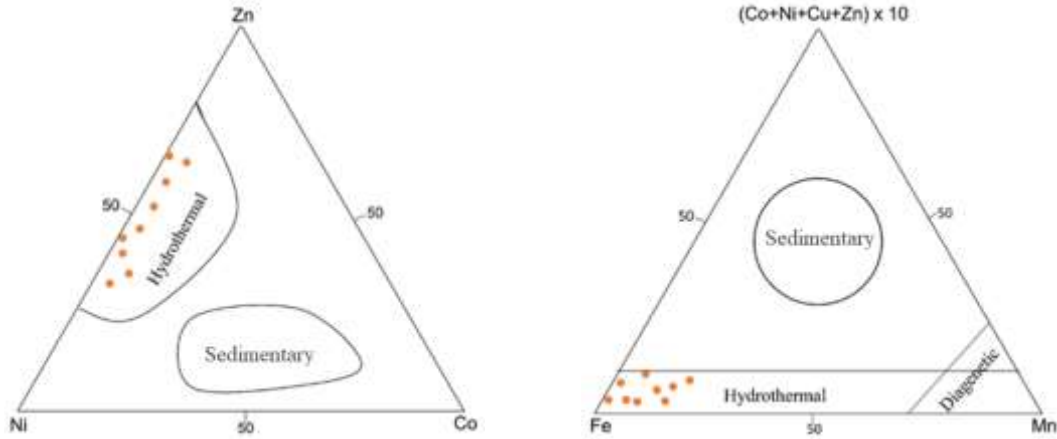


Figure 9 (Ni-Zn-Co) ternary plot of auriferous deformed/remobilized quartz veins **Figure 10** (Co+Ni+Cu+Zn)-Fe-Mn ternary plot of auriferous deformed/remobilized quartz veins

Au, Ag, Fe, Cu, Zn, As and Pb were analyzed by atomic absorption spectrometry (AAS). This method yields very high-quality data for these elements (Nurmi et al., 1991) with detection limits of 0.01ppm. The concentration of Au varies from 1.54 to 7.55 ppm, and the concentrations of associated elements in auriferous deformed/ remobilized quartz veins are shown in Table 5. Pearson correlation coefficient values of Au and associated elements in auriferous deformed/ remobilized quartz veins are shown in Table 6.

Table 5 The concentration of Au and associated elements in auriferous deformed/ remobilized quartz veins

| | Au | Ag | Fe | Cu | Zn | As | Pb |
|--------|-----------|-----------|-----------|-----------|-----------|-----------|-----------|
| TNQD-1 | 7.01 | 8.77 | 154320 | 32500 | 10 | 10 | 5 |
| TNQD-2 | 1.54 | 0 | 72800 | 17500 | 11 | 14 | 9 |
| TNQD-3 | 4.72 | 1.1 | 29220 | 37021 | 17 | 9 | 0 |
| TNQD-4 | 3.55 | 4.25 | 95940 | 22560 | 13 | 11 | 18 |
| TNQD-5 | 2.12 | 0.37 | 56700 | 21250 | 20 | 3 | 0 |
| TNQD-6 | 2.15 | 0 | 32090 | 24472 | 30 | 12 | 0 |
| TNQD-7 | 4.51 | 7.81 | 73170 | 36880 | 23 | 5 | 12 |
| TNQD-8 | 1.61 | 0.085 | 47970 | 16770 | 15 | 8 | 0 |
| TNQD-9 | 7.55 | 5.56 | 166200 | 31330 | 19 | 3 | 0 |

Table 6 Pearson correlation coefficient values of Au and associated elements in auriferous deformed/ remobilized quartz veins

| Proximity Matrix | | | | | | | |
|-------------------------|--------------------------|-----------|-----------|-----------|-----------|-----------|-----------|
| Case | Matrix File Input | | | | | | |
| | Au | Ag | Fe | Cu | Zn | As | Pb |
| Au | 1 | | | | | | |
| Ag | 0.826 | 1 | | | | | |
| Fe | 0.802 | 0.743 | 1 | | | | |
| Cu | 0.711 | 0.653 | 0.251 | 1 | | | |
| Zn | -0.228 | -0.194 | -0.415 | 0.19 | 1 | | |
| As | -0.262 | -0.276 | -0.247 | -0.325 | -0.274 | 1 | |
| Pb | -0.03 | 0.406 | 0.177 | -0.014 | -0.335 | 0.319 | 1 |

Ag, Fe and Cu are strongly correlated with Au. As and Pb are moderately correlated with each other (Table 6). Analysis of the geological data from the auriferous deformed/ remobilized quartz veins shows two distinct geological associations: (1) Au, Ag, Fe and Cu and (2) Pb and As, and Zn is not correlated with other elements.

Minor Elements in Pyrite

The Co and Ni ratio in pyrite appears to have been used to distinguish magmatic, hydrothermal and sedimentary origins of pyrites in ore deposition (Loftus-Hills and Solomon, 1967; Bralía et al., 1979; Bajwah et al., 1987; Brill, 1989). The Co/Ni ratio for magmatic pyrites is greater than 5 in most cases, and in some greater than 10 (Bralía et al., 1979; Bajwah et al., 1987). The Co and Ni contents and the Co/Ni ratios in hydrothermal pyrites vary greatly; the Co and Ni contents can reach up to 1000ppm, and the Co/Ni ratios are generally greater than 1 and can show much variation. Sedimentary pyrites are generally characterized by low contents of Co and Ni and a Co/Ni ratio < 1. Generally, Co contents, which are less than 100ppm, are less than Ni contents (Chen et al., 1987).

Xuexin (1984) mentioned a statistically significant difference among sedimentary, hydrothermal (replacement veins), and massive sulphide pyrites (Table 7). According to his study, the massive sulphide pyrites are characterized by a Co:Ni ratio between 5 and 50; hydrothermal pyrites by a variable Co:Ni ratio (often less than 5); and sedimentary pyrites by a much lower Co:Ni ratio (typically < 1). Pyrite from sulphide ore deposits generally contains appreciable amounts of cobalt and has Co > Ni.

Table 7 Geometric means of cobalt (Co) and nickel (Ni) contents (in ppm) and Co:Ni ratios of sediment, hydrothermal, and massive sulphide pyrite minerals (Xuexin, 1984)

| No. | Type of Pyrite | Co | Ni | Co:Ni |
|-----|--|-----|-----|-------|
| 1 | Sedimentary | 41 | 65 | 0.8 |
| 2 | Volcano-Hydrothermal, Metamorphosed and Skarn-Hydrothermal | 141 | 121 | 2-3 |
| 3 | Volcanogenic Massive Sulphide | 486 | 56 | 3.5 |

According to Carstens (1942), pyrite of sedimentary origin is characterized by containing less than 100 ppm cobalt and Co < Ni, whereas pyrite of hydrothermal origin has 400-2400 ppm cobalt and Co > Ni. Pyrite from high-temperature deposits is generally high in cobalt, but noted exceptions and considered that the effect of temperature was slight. Pyrite of high-temperature and hydrothermal sulphide deposits has only a slightly higher average nickel content than pyrite of sedimentary origin and the ranges of concentration overlap. Hawley (1952) found that Ni content was a little higher in high-temperature samples.

In the study area, 20 pyrite minerals were detected by SEM-EDX to know the elemental composition. The Co and Ni contents of ore-bearing pyrites from the Taung Ni gold prospect range from 0.33-0.78wt% and 0.13-0.36wt%, respectively. Average contents of Co and Ni are 0.526wt% and 0.195wt%, respectively. (Table 8). Average content of Co (0.526 wt.%) is higher than Ni content (0.195 wt.%) and it shows that their origin may be of hydrothermal origin. Average ratio for Co/Ni is 2.698. It indicates that pyrites from Taung Ni gold prospect area may be formed under the hydrothermal conditions.

Table 8 SEM-EDX analyses of element composition (wt.%) of pyrite minerals. Element composition (normalized wt.%) of pyrite minerals

| No. | Samples | Fe(wt%) | S(wt%) | Co(wt%) | Ni(wt%) | Co/Ni |
|-----|----------------|---------|--------|----------------|--------------|----------------|
| 1 | TNP-1 | 43.23 | 55.65 | 0.78 | 0.36 | 2.166667 |
| 2 | TNP-2 | 45.89 | 53.36 | 0.55 | 0.2 | 2.75 |
| 3 | TNP-3 | 45.02 | 54.3 | 0.53 | 0.15 | 3.533333 |
| 4 | TNP-4 | 45.25 | 54.23 | 0.39 | 0.13 | 3 |
| 5 | TNP-5 | 43.21 | 55.91 | 0.65 | 0.23 | 2.826087 |
| 6 | TNP-7 | 44.78 | 54.74 | 0.33 | 0.15 | 2.2 |
| 7 | TNP-9 | 43.56 | 55.74 | 0.5 | 0.2 | 2.5 |
| 8 | TNP-10 | 45.23 | 54.15 | 0.48 | 0.14 | 3.428571 |
| | Average | | | 0.52625 | 0.195 | 2.69872 |

Gold Fineness

Gold occurs generally in the native state and is the most abundant of all the gold minerals. It usually occurs associated with a little quantity of silver. The silver content of gold is commonly given as fineness (Gold Fineness- 1000 Au/Au+Ag) (Fisher, 1945). Fisher (1950) concluded that fineness used with other criteria furnishes a sensitive and reliable guide to the relative temperature of ore formation, at least within the epithermal and the upper part of the mesothermal range of temperatures. The fineness of epithermal gold is from 500 to 700. Near the bottom of the epithermal zone (corresponding to the leptothermal zone of Graton, 1933), the fineness is about 700 and may be as much as 800. The fineness of mesothermal gold varies from 750 to 900, with 850-870 being common. The fineness of hypothermal gold is always greater than 800. Fineness of 900 or more results from oxidation under conditions favouring the removal of silver. According to Morrison et al. (1991) the major deposit classes are characterized by the overall average range of deposits and total range of gold fineness values as follows: Archaean 700±1000 (780±1000); slate belt 920(800±1000); plutonic 825 (650±970); porphyry 700±1000 (650±1000); volcanogenic 650±850 (520±870); epithermal 440±1000 (0±1000). The major deposit classes are characterized by the overall average or range of averages and total range of gold fineness (After Fisher, 1950 and Morrison et al., 1991) (Table 9).

Gold fineness was calculated in the study area, based on the result of SEM-EDX analysis. Gold fineness of SEM-EDX analysis of electrum grains is shown in Table.10. It ranges from 771.2 to 795 with average gold fineness of 779.14. Gold fineness of SEM-EDX analysis of gold grains is shown in Table.11. It ranges from 826.2 to 881.3 with average gold fineness of 851.94.

The gold fineness showed two ranges: (1) high fineness (826.2 - 881.3) and (2) low fineness (771 - 795). It suggests that Au was remobilized and recrystallized during later stages.

Table 9 Overall average, range of averages and range of fineness for major deposit lasses (After Fisher, 1950 and Morrison et al., 1991)

| Deposit Types | Overall Average /Range of Averages | Total Range |
|---------------|------------------------------------|-------------|
| Archean | 940 | 780 ± 1000 |
| Plutonic | 825 | 650 ± 970 |
| Porphyry | 700 ± 1000 | 650 ± 1000 |
| Volcanogenic | 650 ± 850 | 520 ± 870 |
| Slate belt | 920 | 800 ± 1000 |
| Hypothermal | | 925 |
| Mesothermal | 850 ± 870 | 750 ± 900 |
| Epithermal | 440 ± 1000 | 0 ± 1000 |

Table 10 Gold Fineness of SEM-EDX analysis of electrum grains

| No. | Element | Au (wt%) | Ag (wt%) | Gold Fineness | Remark |
|---------|---------|----------|----------|---------------|----------|
| 1 | Grain 1 | 77.12 | 22.88 | 771.2 | Electrum |
| 2 | Grain 2 | 77.84 | 22.16 | 778.4 | Electrum |
| 3 | Grain 3 | 79.5 | 20.5 | 795 | Electrum |
| 4 | Grain 4 | 76.91 | 23.09 | 769 | Electrum |
| 5 | Grain 5 | 78.2 | 21.8 | 782 | Electrum |
| Average | | 77.914 | 22.086 | 779.14 | |

Table 11 Gold Fineness of SEM-EDX analysis of gold grains

| No. | Element | Au (wt%) | Ag (wt%) | Gold Fineness | Remark |
|---------|----------|----------|----------|---------------|--------|
| 1 | Grain 1 | 82.62 | 17.38 | 826.2 | Gold |
| 2 | Grain 2 | 85.32 | 14.68 | 853.2 | Gold |
| 3 | Grain 3 | 85.05 | 14.95 | 850.5 | Gold |
| 4 | Grain 4 | 87.5 | 12.5 | 875 | Gold |
| 5 | Grain 5 | 84.03 | 15.97 | 840.3 | Gold |
| 6 | Grain 6 | 82.86 | 17.14 | 828.6 | Gold |
| 7 | Grain 7 | 84.19 | 15.81 | 841.9 | Gold |
| 8 | Grain 8 | 83.62 | 16.38 | 836.2 | Gold |
| 9 | Grain 9 | 84.18 | 15.82 | 841.8 | Gold |
| 10 | Grain 10 | 88.13 | 11.87 | 881.3 | Gold |
| 11 | Grain 11 | 87.1 | 12.9 | 871 | Gold |
| 12 | Grain 12 | 87.73 | 12.27 | 877.3 | Gold |
| Average | | 85.19 | 14.81 | 851.94 | |

Fluid Inclusion Geochemistry

In the study area, based on the number of phases present at room temperature (Shepherd et al., 1985) and their microthermometric features, two fluid inclusion types were recognized: Type I monophasic aqueous inclusions (L=Liquid), and Type II two-phase (L=Liquid+V=Vapour) aqueous inclusions. Type II is more abundant of the two inclusion types.

Monophasic aqueous inclusions (Type I) of fluid inclusions occur in both quartz veins and are characterized by single phase (liquid or gas) at room temperature. Aqueous two-phase fluid inclusions (Type II) are also seen in both gold-bearing sulphide quartz veins, and deformed quartz veins by a vapour bubble in an aqueous liquid at room temperature with transparency and low relief.

In sulphide-bearing veins (Early Stage), both ice melting and homogenization temperature can be measured and it ranges from 340°C to 403°C and melting temperature ranges from -1.7 to -2.0 (NaCl equiv. wt.% range from 3.01 to 3.53).

In deformed quartz vein (Later Stage), it also has bi-phase inclusions, homogenization temperature can be measured, the range of melting temperature is from -1.3 °C to -1.6 °C and salinity NaCl equiv. wt. % is from 2.31 to 2.83. Homogenization temperature is 320°C to 396°C.

From fluid inclusion data of mineralized quartz veins, it can be deduced that there are two different mineralization phases marked by difference of homogenization temperature and salinity. Fluid inclusion microthermometry data of selected samples is shown in Table 12. Temperature-salinity diagram for various types of ore deposits (Wilkinson, 2001) is shown in Figure 11.

Table 12 Fluid inclusion microthermometry data of selected samples

| Sample ID | Host Rock | Host Mineral | Inclusion Type | No. of Inclusion | Homogenization Tem, Range (°C) | Ice Melting Tem (°C) | Salinity (wt% NaCl) | Remarks |
|-----------|-----------|--------------|----------------|------------------|--------------------------------|----------------------|---------------------|------------------------------------|
| PYT-1 | quartzite | quartz | L-V | 11 | 340-403 | -1.7 to -2 | 3.01 to 3.53 | Sulphide quartz vein (Early Stage) |
| PYT-2 | quartzite | quartz | L-V | 10 | 320-396 | -1.3 to -1.6 | 2.31 to 2.83 | Deformed quartz vein (Later Stage) |

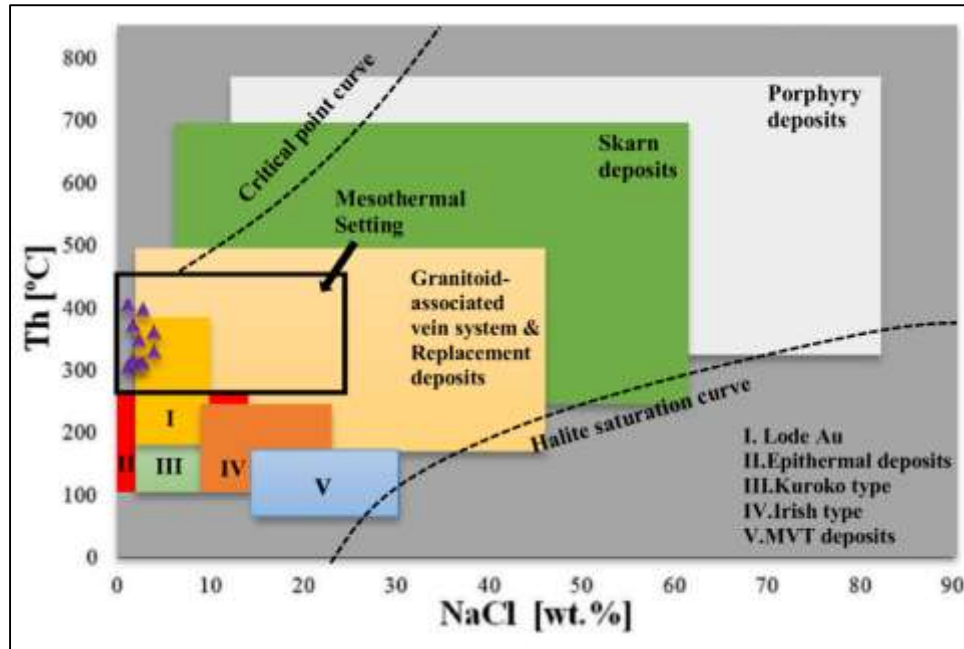


Figure 11 Temperature-salinity diagram for various types of ore deposits (Wilkinson, 2001)

Conclusion

At Taung Ni gold prospect, two types of veins system are found: (1) gold-bearing sulphide quartz vein and (2) auriferous deformed/remobilized quartz vein in strongly brecciated and oxidized zone. In both types of quartz veins, Pearson statistical analyses confirm a strong negative correlation between SiO_2 and other major oxides. The results indicate that the quartz veins were of hydrothermal origin. In both types of quartz veins, the Si-Al discrimination diagram, (Ni-Zn-Co) ternary plot and (Co+Ni+Cu+Zn)-Fe-Mn ternary plot indicate that the quartz veins bearing gold are of hydrothermal origin. In gold-bearing sulphide quartz veins, Ag, As, Bi, Cu, S, Se and Te are strongly correlated with Au. These correlations show that the mineralization indicates the complex nature of hydrothermal system. In auriferous deformed/ remobilized quartz veins, Ag, Fe and Cu are strongly correlated with Au. In the study area, the Co and Ni contents in pyrite show $\text{Co} > \text{Ni}$ and the average ratio for Co/Ni is 2.698. It indicates that pyrites from Taung Ni gold prospect area may be formed under the hydrothermal conditions. The gold fineness shows two ranges: (1) high fineness (826.2 - 881.3) and (2) low fineness (771 - 795). It suggests that Au was remobilized and recrystallized during late stages. Gold mineralization in veins shows two generations as indicated by gold fineness probably suggesting multiple gold depositions. Gold fineness indicates that the Taung Ni gold prospect was formed with the mesothermal setting. From fluid inclusion data of mineralized quartz veins, it can be recognized that there are two different mineralization phases marked by difference of homogenization temperature and salinity. In sulphide bearing vein (Early Stage), homogenization temperature can be measured and it ranges from 340°C to 403°C and melting temperature ranging from -1.7 to -2.0 , salinity NaCl equiv. wt.% range from 3.01 to 3.53. In deformed quartz vein (Later Stage), it also has bi- phase inclusions, the range of melting temperature is from -1.3°C to -1.6°C and salinity NaCl equiv. wt. % is from 2.31 to 2.83. Homogenization temperature is 320 to 396°C . Therefore, it suggests that the Taung Ni gold prospect is considered to be consistent with mesothermal setting.

Acknowledgements

I am deeply grateful to U Than Htay, Deputy Director General (Retired), Department of Geological Survey and Mineral Exploration, Ministry of Mines for his critical reading and improvement of the manuscript.

References

- Aung Ye Ko, Day Wa Aung and Ohn Thwin, (2018c) "Petrography and Mineralogical, Geochemical Investigations of Metamorphic Rocks in Taung Ni Area, Madaya Township, Mandalay Region". *Universities Research Journal 2018, Vol. 11, No.11. University of Yangon, Myanmar.* P 203-224.
- Bajwah, Z.U., Seccombe, P. K., & Offier, R., (1987) "Trace element distribution, Co: Ni ratios and genesis of the Big Cadia iron-copper deposit, New South Wales, Australia". *Mineralium Deposita*, 22(4), 292-300.
- Bonatti, E., Kraemer T., and Rydell H.S., (1972c) "Classification and genesis of submarine iron - manganese deposits. In Ferromanganese Deposits on the Ocean Floor". *IDOE, Columbia University, New York*, pp.149-166.
- Bralia, A., Sabatini, G. & Troja, F., (1979) "A revaluation of the Co/Ni ratio in pyrite as geochemical tool in ore genesis problems: evidences from southern Tuscany pyritic deposits". *Mineralium Deposita*, 14(3), 353-374.
- Brill., B. A., (1989) "Trace element contents and partitioning of elements in ore minerals from the CSA Cu-Pb-Zn deposit, Australia". *Canadian Mineralogist*, 27(2), 263-274.
- Carstens, C.W. (1942) "Uber den Co-Ni-Gehalt norwegischer Schwefelkies-vorkommen: Kgl". *Norske Videnskabs, Selgkabs, Forh.* 15: 165–168.
- Chen, G. Y., (1987) "Genetic mineralogy and prospecting mineralogy". *Chongqing Publishing House, Chongqing*, 874pp.
- Choi, J.M., and Hariya Y., (1992) "Geochemical study of manganese oxide deposits in the Setana area, south western Hokkaido, Japan". *Mining Geology*, 42, 165-173.
- Fisher, N. H., (1945) *The fineness of gold, with special reference to the Morobe gold field*: Econ. Geology, v. 40, p. 449-495 and 537-563.
- Fisher, N. H., (1950) "Application of gold fineness to the search for ore": *Australasian Inst. Mining and Metallurgy Proc.* 156-157, p. 185-190.
- Graton, L. C., (1933) "The depth-zones in ore deposition": *Econ Geology*, v. 28, p. 513- 555.
- Hawley, J.E., (1952) "Spectrographic studies of pyrite in some Eastern Canadian mines", *Economic Geology* 47: 260–304.
- Khin Maung Shwe., 1973. *The Geology of Sedaw-Taung Gaung Area, Mandalay District*. M.Sc Thesis, Department of Geology, University of Mandalay (Unpublished)
- Loftus-Hills, G. & Solomon, M., (1967) "Cobalt, nickel and selenium in sulphides as indicators of ore genesis". *Mineralium Deposita*, 2(3), 228-242.
- Morrison, G.W., Rose, W.J., and Jaireth, S., (1991) "Geological and geochemical controls on the silver content (fineness) of gold in gold- silver deposits". *Ore Geology Reviews*, Vol.6: pp. 333-364.
- Nurmi, P. A., Lestinen, P. & Niskavaara, H. (1991) Geochemical characteristics of mesothermal gold deposits in the Fennoscandian Shield, and a comparison with selected Canadian and Australian deposits. Geological Survey of Finland, Bulletin 351. 101 p.
- Peters, T., (1988) "Geochemistry of manganese - bearing cherts associated with Alpine ophiolites and the Hawasina formations in Oman," *Marine Geology*, vol. 84, no. 3-4, pp. 229–238, 1988.
- Shah, M.T., and Khan A., (1999) "Geochemistry and origin of Mn-deposits in the Waziristan ophiolite complex, north Waziristan, Pakistan". *Mineralium Deposita*. P.697-704.
- Theodore, T.G., Bornhorst, Pekka A., (1998) "Nurmi and Olavi Kontoniemi Geochemistry of gold and associated elements in the Paleoproterozoic Osikonmaki gold deposit, southeastern Finland". *Geological Survey of Finland, Special Paper* 25.81 - 90.
- Wilkinson, J.J., (2001) Fluid inclusions in hydrothermal ore deposits. *Lithos* 55: 229–272.
- Xuexin, S., (1984) "Minor Elements and Ore Genesis of the Fankou Lead-Zinc Deposit, China". *Mineral Deposita* 19: 95 104.